

## Molecular-dynamics simulation of Al/SiC interface structures

Xuan Luo,\* Gefei Qian,\* and E. G. Wang

*State Key Laboratory for Surface Physics, and Institute of Physics & Centre for Condensed Matter Physics, Chinese Academy of Science, Beijing, 100080, People's Republic of China*

Changfeng Chen

*Department of Physics, University of Nevada, Las Vegas, Nevada 89154*

(Received 22 September 1998)

Molecular-dynamics simulation employing Tersoff and Ito-Kohr-Das Sarma potentials has been performed to study structural properties of Al/SiC interfaces. The atomic configuration and cohesive energy of various Al/SiC interfaces formed between low-index planes of Al and SiC surfaces have been calculated. A positive correlation between the existence of a specific orientation relationship (OR) and its cohesive energy has been identified and used as a guide in search of more Al/SiC OR's. Structural disorder is induced by the interfacial bonding dominated by the Al-C interaction, but is limited to a narrow region near the interface, thus maintaining definite OR's between Al and SiC. It is shown that the cohesive energy decreases only slightly when the OR's deviate from the ideal arrangement within a small range, suggesting the stability of these nonideal OR's. The calculated results are in good agreement with experiment and provide an atomic-level description for the low-index Al/SiC interfaces. [S0163-1829(99)10115-2]

### I. INTRODUCTION

The study of metal/semiconductor interfaces has received considerable attention<sup>1-8</sup> because of their wide-range applications in electronic devices and composite materials. The Al/SiC interfaces provide a prototypical example that combines fundamental scientific interests and practical technological applications.  $\beta$ -SiC is a good candidate for device application in high-temperature and high-radiation environments and Al is used both in forming contacts on SiC devices<sup>3</sup> and as a matrix material in SiC whisker-reinforced composites.<sup>2</sup> The  $\beta$ -SiC whisker-reinforced aluminum composites (Al/SiCw) can be used as structure materials in the automobile and aerospace industry and also in some demanding environments such as the first wall of a fusion reactor. The properties of Al/SiCw composites are strongly influenced by the structure of the reinforcing phase SiC whisker and the Al matrix. Therefore, systematic experimental and theoretical studies of interfaces between SiC and Al are of great technological interest. There is also fundamental scientific issues concerning atomic-level descriptions of such interfaces that need to be addressed.

Many experimental studies<sup>2,9-20</sup> on the Al/SiC interface have been performed. Most of them observed orientation relationship (OR) between Al and SiC in either  $\alpha$ -SiC particulates reinforced Al or  $\beta$ -SiC whisker-reinforced Al composites. Van Den Burg and De Hosson<sup>9</sup> studied SiC particulates-reinforced aluminum composite interface structure and found an orientation relationship,  $[2\bar{1}\bar{1}0]_{\text{SiC}} \parallel [110]_{\text{Al}}$ ,  $(0001)_{\text{SiC}} \parallel (111)_{\text{Al}}$ . Arsenault<sup>10</sup> and Romero<sup>11</sup> found a specific crystallographic orientation in the Al/ $\alpha$ -SiC interfaces,  $[11\bar{2}0]_{\text{SiC}} \parallel [110]_{\text{Al}}$ ,  $(0001)_{\text{SiC}} \parallel (\bar{1}12)_{\text{Al}}$ . On the SiC whisker-reinforced aluminum matrix composites, various experimental results have shown that there is no reaction between Al and SiC, and no

long distance mutual diffusion at the Al/SiC interface,<sup>12</sup> and crystal OR's exist between the Al matrix and the SiC whisker.<sup>13,14</sup> A detailed study<sup>21</sup> shows that most of the OR's are not very strict but there is a small deviation from the ideal OR.

On the theoretical side, attempts have been made to study interfaces between SiC and metals. Using charge self-consistent extended Hückel theory, the adsorption of Au on  $\beta$ -SiC(111) surface has been studied<sup>22</sup> and the results that the Au-Si interaction is stronger than the Au-C interaction agree qualitatively with experiment. The electronic structures of Ti/ $\beta$ -SiC interface<sup>1</sup> and Ti, Cu, Pd/ $\alpha$ -SiC interfaces<sup>23</sup> have been studied using the atom superposition and electronic delocalization molecular-orbital method. The results show that all these metals bind strongly to the silicon carbide surfaces. There has been also work reported on the study of Al/SiC interfaces.<sup>24-28</sup> Li, Arsenault, and Jena<sup>24</sup> used a quantum-chemical method to calculate the total energies of Al(111)  $[110] \parallel \alpha$ -SiC(0001)  $[2\bar{1}\bar{1}0]$  and Al(100)  $[110] \parallel \beta$ -SiC( $2\bar{1}\bar{1}$ )  $[111]$  interfaces. They conclude that the bond strength between SiC and Al could be stronger than the bond between Al and Al and the adhesive energy between the biggest-side surface  $\beta$ -SiC( $2\bar{1}\bar{1}$ )/Al is larger than that between the top-surface  $\beta$ -SiC(111)/Al. Rao and Jena<sup>25</sup> calculated the bond lengths and binding energies of Al-Al, Al-Si, Al-C, and Si-C dimers by a self-consistent quantum-mechanical method. They found that the binding energy of Al-C is larger than that of Al-Si. The results can be used to understand the nature of the atomic bonding at the interface. Lu, Zhang, and Xie<sup>26</sup> used a cluster model to describe the adsorption of Al on the  $\beta$ -SiC (100) surfaces. They found that the Al-SiC interaction is limited to a narrow region near the interface. The adsorption of Al on the Si-terminated (100) surface hardly affects the Si-C bond, whereas the adsorption of Al on the C-terminated (100) surface weakens the

Si-C bond. The Al-C interaction is stronger than the Al-Si interaction. Kohyama<sup>27</sup> used an *ab initio* pseudopotential method and the CG electronic-minimization techniques by Bylander, Kleinman, and Lee<sup>29</sup> to study the SiC(110)-Al(110) interfaces. The main conclusion is that the Al-C interactions at the interfaces have features different from those of Al-Si interactions and the electron-density distribution between the Al and C atoms are similar to those of the Si-C bond. He concluded that the strong attractive C-Al interactions with covalent and ionic characters should play a favorable role in the adhesion between SiC and Al surfaces. Hu, Yan, and Ohuchi<sup>28</sup> employed a tight-binding method to investigate surface electronic structures of the  $\beta$ -SiC reconstructed (001) surfaces and the Al/ $\beta$ -SiC (001) interfaces. Their results indicate that Al deposition on the  $\beta$ -SiC (001) surface may induce the substrate to return to the ideal unreconstructed surface and that the Al-C interaction is stronger than the Al-Si interaction. Al deposition on C-terminated surfaces may form a better bonded interface than that on the Si-terminated surfaces.

Most of recent studies mentioned above have focused on the electronic structure to reveal the binding mechanism at Al/SiC interfaces. Although electronic structure calculations can explain the charge transfer and the bond-strength characteristics, they do not directly address the issue of interface structures. In particular, the experimentally observed OR's at Al/SiC interfaces<sup>13,14,21</sup> and the deviation from the ideal OR's in Al/SiCw composites<sup>21</sup> are still to be understood from an atomic-level description. To this end, it is necessary to carry out large-scale systematic investigation of the atomic configurations at the interface. Molecular-dynamics (MD) simulations employing empirical potentials are well suited for such problems. It can provide a precise picture of the atomic arrangements at the interface that include a large number of atoms per unit cell and the surface reconstruction. In this respect, first-principles calculations still have difficulties.<sup>24,27</sup> In this paper, we report a systematic MD simulation of Al/SiC interfaces with an emphasis on the study of OR's. Although semiempirical and semiquantitative, our study represents the first attempt to provide a systematic description for Al/SiC interface structures. Calculations are carried out for various crystallographic orientations as well as for deviation from the ideal orientation relationships at the interface. This work complements first-principle calculations<sup>27</sup> and semiempirical tight-binding studies<sup>26</sup> by including a much larger numbers of atoms in the simulation.

This paper is organized as follows. The description of the method is presented in Sec. II, where we give the structural models of the Al/SiC interfaces and discuss the choice of the potential parameters used in the MD calculations. The results are presented in Sec. III. Finally, a summary is given in Sec. IV.

## II. METHODS

### A. The potentials

In this paper, we have employed two widely used potential formalisms proposed by Tersoff<sup>30</sup> and by Ito, Khor, and Das Sarma.<sup>31-33</sup> Below, we briefly summarize these formalisms and discuss their implementation in the present calculations.

The Tersoff potential formalism is

$$V_{ij} = f_c(r_{ij})[f_R(r_{ij}) + b_{ij}f_A(r_{ij})], \quad (1)$$

where  $f_R$  and  $f_A$  represent the repulsive and attractive atom pair interactions, respectively.

$$f_R(r_{ij}) = A_{ij}e^{-\lambda_{ij}r_{ij}}, \quad f_A(r_{ij}) = B_{ij}e^{-\mu_{ij}r_{ij}}, \quad (2)$$

where  $\lambda_{ij}$  and  $\mu_{ij}$  are positive,  $A_{ij}$  and  $B_{ij}$ , both positive, are modified repulsive and attractive terms, and  $f_c$  is an optional cutoff function to define the interaction range. The  $b_{ij}$  function modulating the attractive interaction has an explicit bond-angle dependence and includes many-body interactions.

$$b_{ij} = \chi_{ij}(1 + \beta_i^{n_i} \xi_{ij}^{n_i})^{-\frac{1}{2n_i}} \quad (3)$$

$$\xi_{ij} = \sum_{k \neq i,j} f_c(r_{ik})g(\theta_{ijk}) \quad (4)$$

$$g(\theta_{ijk}) = 1 + c_i^2/d_i^2 - c_i^2/[d_i^2 + (h_i - \cos \theta_{ijk})], \quad (5)$$

where  $\chi_{ij}$  is a mixture parameter to strengthen or weaken the heteropolar bonds,  $h_i$  is formally the cosine of the energetically optimal angle,  $d_i$  determines how sharp the dependence on angle is,  $c_i$  determines the strength of the angular effect,  $n_i$  and  $\beta_i$  are parameters to adjust the strength of  $b_{ij}$ .

The Tersoff potential has been successfully applied to the study of Si and SiC systems.<sup>34</sup> We have employed the Tersoff potential to study the low-index SiC surfaces in a recent work<sup>35</sup> and have found some interesting surface relaxation and reconstruction patterns in good agreement with experiment and other calculations. We have adjusted the cutoff parameter for the surface C atoms to extend the range of the interactions. This is because the interaction between the second-neighbor surface atoms must be considered to account for some surface structural features such as the surface dimer row.<sup>36</sup> More details on the parameters used for SiC can be found in Ref. 35. The fully relaxed SiC surface configurations obtained in that work have been used to represent the SiC surface as the starting point in the simulation reported in the present work.

For the simulation involving Al, we have used the Ito-Khor-Das Sarma potential given by the formalism<sup>31-33</sup>

$$V_{ij} = A \exp[-\beta(r_{ij} - R_i)^\gamma] \left\{ e^{-\theta r_{ij} - \frac{B_0}{Z_i^\alpha}} \times e^{-\lambda r_{ij}} \left[ 1 + \sum_{k \neq i,j} (\cos \eta(\theta_{jik} - \theta_i) - 1) \right] \right\}, \quad (6)$$

where  $\theta_i$  is the equilibrium angle between nearest-neighbor bonds for a regular structure with coordination number  $Z_i = \sum_j \exp[-\beta(r_{ij} - R_i)^\gamma]$ ,  $\theta_{ijk}$  is the angle between bonds  $ij$  and  $ik$ ,  $\eta$  is a parameter to fit the bond-bending force constant, and the summation is only over nearest-neighbor atoms whose bond  $ik$  is equal to the nearest bonds of  $ij$ .  $R_i$  is the minimum interatomic distance of these neighbors. The quantity  $\exp[-\beta(r_{ij} - R_i)^\gamma]$  is the counterpart of the Tersoff's bare bonding potential. The parameters  $\beta$  and  $\gamma$  can be fitted to give the correct effective coordination numbers.

TABLE I. Potential parameters for Al-Si and Al-C.

|       | A (eV)    | $B_0$ (eV) | $\theta$ ( $\text{\AA}^{-1}$ ) | $\lambda$ ( $\text{\AA}^{-1}$ ) | $\beta$ | $\gamma$ | $\alpha$ |
|-------|-----------|------------|--------------------------------|---------------------------------|---------|----------|----------|
| Al-C  | 8165.3588 | 0.03953    | 3.9238                         | 1.9619                          | 33.5313 | 3.2707   | 0.4042   |
| Al-Si | 4265.9784 | 0.04714    | 3.7478                         | 1.8739                          | 23.8234 | 3.4078   | 0.6737   |

The Al-Al parameters are taken from Ref. 33 and the C-C and Si-Si parameters are from Ref. 31. As for the parameters of the Al-C and Al-Si interactions, we took the average of the corresponding single-element values for parameters  $B_0$ ,  $\lambda$ ,  $\beta$ ,  $\gamma$ ,  $\alpha$  and optimized more sensitive parameters  $A$  and  $\theta$  according to the bond length and the binding energy.<sup>25</sup> The parameter  $\eta$  is set to zero for the Al-C and Al-Si interactions as in the Al-Al case<sup>33</sup> because there is no definite bond angle between Al-C, Al-Si, and Al-Al. The potential parameters for Al-C and Al-Si used in our simulation are listed in Table I.

### B. The structural model

In this paper, we first studied the five interfaces reported in a recent scanning tunnelling electron microscope (STEM) experiment,<sup>13</sup> followed by a systematic study of fifteen low-index Al/SiC interfaces formed between Al (100), (110), (111), and  $\beta$ -SiC with relaxed (100), (110), (111) surfaces. All these Al/SiC interfaces are assumed to have ideal orientation relationships.

The MD simulation cells are constructed by choosing the contacting Al and SiC surfaces with a small misfit ratio and an appropriate thickness to represent the semi-infinite Al and SiC bulk crystals. Here we describe the case of  $(100)_{\text{SiC}} \parallel (100)_{\text{Al}}$ ,  $[100]_{\text{SiC}} \parallel [100]_{\text{Al}}$  as an example to illustrate the procedure of constructing the MD cells. We selected a square SiC surface area of  $13 \times 13$  SiC unit cells to match a square Al surface area of  $14 \times 14$  Al unit cells, with a misfit ratio of only 0.08%. In the direction normal to the interface, we chose eight layers of Al plus eight layers of SiC. The total number of atoms in the MD cell is about 10,000. The distance between the contacting surfaces of Al and SiC was first set to the previously obtained<sup>25</sup> Al-C bond length for Al/SiC-C interfaces and the Al-Si bond length for Al/SiC-Si interfaces and the average of the Al-Si and Al-C bond lengths between Al and the nonpolar SiC(110) surface. It is then optimized by maximizing the cohesive energy of the system and used as the starting point of the MD simulation. The bottom two layers of SiC and the top three layers of Al were fixed to simulate the two semi-infinite bulk, while other layers were set to relax freely. Periodic boundary conditions were applied to the four boundary planes. All other MD cells were constructed in the same way, although the exact dimensions of the contacting surfaces vary for different OR's.

Another subject of great interest is the observation that many experimentally observed OR's deviate from ideal arrangement.<sup>21</sup> To address this issue, we study the stability of the OR's of Al/SiC interfaces with regard to changes in relative orientation. We focus on the case of  $(100)_{\text{Al}} \parallel (100)_{\text{SiC}}$ ,  $[100]_{\text{Al}} \parallel [100]_{\text{SiC}}$ . The orientation is varied by rotating bulk Al about two axes normal and parallel to the interface. These rotations can be expressed in terms of two Euler angles  $\psi$  and  $\theta$ . In this situation, the MD cell is

similar to those described above for ideal OR's, but with some notable differences. After the rotation of Al bulk, we cut an Al box with the contacting surface matching that of the SiC surface. Rigid boundary conditions<sup>37</sup> are used, in which the four lateral boundaries were replaced by heavy walls.<sup>37-39</sup> The atoms inside the wall are allowed to relax freely, while the atoms on the walls remain rigid. Using this model, we calculated the cohesive energy for a series of OR's with different Euler angles. It should be pointed out that the rigid boundary conditions may make the cohesive energy higher than that using the periodic boundary conditions because it introduces artificial confinement. This should not be disturbing, however, since we are interested here in the comparison of relative cohesive energies corresponding to different rotation angles.

### C. The simulation procedure

The simulation in this work has employed a constant number-volume-temperature ensemble containing about 10 000 atoms in various MD cells. The starting atomic configurations were composed of a fully relaxed SiC surface<sup>35</sup> and an Al surface with bulk-atomic configurations.

The forces during each time step were defined in terms of the gradient of the potential energy with respect to the length of the vector connecting each pair of atoms and the angle between pairs of the vectors. The positions and velocities of every atom in the MD cell were calculated following each time step by integrating the Newtonian equations of motion using the Verlet algorithm.<sup>40</sup> The time step in the integration is set to 0.3 fs. The potential energies and forces associated with each atom in the MD cell, as well as the total potential energy, the total kinetic energies, the cohesive energies of the Al/SiC interface, and the total maximum force value, were calculated for each time step and atomic configurations were allowed to relax. The calculations were carried out using MD and modified quasidynamic (QD) techniques.<sup>41</sup> The position and velocity of each atom were computed in a fully dynamic mode until both the total potential energy and the total force of the ensemble reached minima at which point the velocity of each atom was set to zero. The system is allowed to evolve further. The procedure was repeated until stable atom positions with approximately zero net force were obtained. The application of both conditions, minima in total potential energy and system force, instead of the standard QD procedure<sup>42</sup> of using a maximum in the kinetic energy for resetting velocities reduces the sensitivity of the calculation to atomic configurations.<sup>43</sup>

The cohesive energy of the Al/SiC interface is defined as

$$\Delta E = (E_{\text{Al}} + E_{\text{SiC}}) - E_{\text{Al/SiC}}, \quad (7)$$

where  $E_{\text{Al}}$  and  $E_{\text{SiC}}$  represent the cohesive energy of bulk Al and SiC, respectively, and  $E_{\text{Al/SiC}}$  represent cohesive energy of the Al/SiC interface.

TABLE II. The orientation relationships observed at the Al/SiC interface by the STEM experiment<sup>13</sup> and the cohesive energy calculated by the present MD simulation.

| Orientation relationship   | Number | Cohesive energy (eV/atom) |
|--|--------|---------------------------|
| $(01\bar{1})_{\text{SiC}} \parallel (001)_{\text{Al}}, [211]_{\text{SiC}} \parallel [100]_{\text{Al}}$       | 14     | 0.394                     |
| $(111)_{\text{SiC}} \parallel (111)_{\text{Al}}, [01\bar{1}]_{\text{SiC}} \parallel [01\bar{1}]_{\text{Al}}$ | 12     | 0.353                     |
| $(111)_{\text{SiC}} \parallel (100)_{\text{Al}}, [01\bar{1}]_{\text{SiC}} \parallel [01\bar{1}]_{\text{Al}}$ | 10     | 0.301                     |
| $(01\bar{1})_{\text{SiC}} \parallel (01\bar{1})_{\text{Al}}, [100]_{\text{SiC}} \parallel [211]_{\text{Al}}$ | 5      | 0.271                     |
| $(01\bar{1})_{\text{SiC}} \parallel (01\bar{1})_{\text{Al}}, [011]_{\text{SiC}} \parallel [211]_{\text{Al}}$ | 3      | 0.181                     |

### III. RESULTS AND DISCUSSION

#### A. Simulation of five OR's observed in the STEM experiment

We first carried out the MD simulation and calculated the cohesive energy for the five OR's reported in the STEM experiment.<sup>13</sup> From the results shown in Table II, it is seen that the probability of observing a given OR increases with its cohesive energy. This result is intuitive and provides a guide in search of more OR's. However, caution should be exercised when making comparison with experimental results. Other factors may alter this simple picture. For example, the calculation of Li *et al.*<sup>24</sup> indicated that the adhesive energy between the side-surface  $\beta$ -SiC( $2\bar{1}\bar{1}$ )/Al is larger than that between the top-surface  $\beta$ -SiC(111)/Al, but in the STEM observation<sup>13</sup> the former OR was not observed. This issue was clarified by another experiment.<sup>19</sup> It was generally accepted that the SiC whiskers have a cubic structure with its [111] axis as the growth direction and the cross section is hexagonal or trigonal surrounded by {211} side planes.<sup>44-46</sup> But these whiskers have many growth faults and are not straight. The above contradiction is due to the fact that the side surface is not an exact {211} plane but composed of fine {111} plane steps.<sup>19</sup> With this cautionary note in mind, we proceed to calculate the cohesive energy of other Al/SiC interfaces and use it as a guide in search of stable OR's under the ideal situation.

#### B. Simulation of 15 low-index Al/SiC interfaces

Experimental results show that the most favorite surfaces of SiC whiskers are (100), (110), (111) surfaces<sup>12</sup> and the common interfaces of Al/SiC are between Al (100), (110), (111) surfaces and SiC (100), (110), (111) surfaces.<sup>13,21</sup> We have carried out MD simulations for 15 Al/SiC interfaces with the crystalline orientation relationships and the cohesive energies listed in Table III. An important observation is that most of the interface structures in Table III have cohesive energies close to those shown in Table II. Based on the above analysis, it is expected that these OR's should also be observable in experiment under ideal situations. In a most recent experimental study,<sup>21</sup> systematic search has yielded all but one OR listed in Table III, along with some other OR's. The only OR not observed is the Al(111)/SiC(110) interface that has the lowest cohesive energy (0.144 eV) among the 15 OR's studied in this paper. This result further supports the use of cohesive energy as a guide in search of more OR's of the Al/SiC interface and other similar systems.

TABLE III. Cohesive energy of the fifteen Al/SiC interfaces studied in this work.

| $\beta$ -SiC | Al    | Orientation relationship   | Cohesive energy (eV/atom) |
|--------------|-------|--|---------------------------|
| (100)-C      | (100) | $(001)_{\text{SiC}} \parallel (001)_{\text{Al}}, [100]_{\text{SiC}} \parallel [100]_{\text{Al}}$             | 0.297                     |
| (100)-C      | (110) | $(100)_{\text{SiC}} \parallel (110)_{\text{Al}}, [001]_{\text{SiC}} \parallel [001]_{\text{Al}}$             | 0.236                     |
| (100)-C      | (111) | $(100)_{\text{SiC}} \parallel (111)_{\text{Al}}, [010]_{\text{SiC}} \parallel [\bar{1}10]_{\text{Al}}$       | 0.303                     |
| (100)-Si     | (100) | $(001)_{\text{SiC}} \parallel (001)_{\text{Al}}, [100]_{\text{SiC}} \parallel [100]_{\text{Al}}$             | 0.199                     |
| (100)-Si     | (110) | $(100)_{\text{SiC}} \parallel (110)_{\text{Al}}, [001]_{\text{SiC}} \parallel [001]_{\text{Al}}$             | 0.131                     |
| (100)-Si     | (111) | $(100)_{\text{SiC}} \parallel (111)_{\text{Al}}, [010]_{\text{SiC}} \parallel [\bar{1}10]_{\text{Al}}$       | 0.242                     |
| (110)        | (100) | $(110)_{\text{SiC}} \parallel (100)_{\text{Al}}, [001]_{\text{SiC}} \parallel [001]_{\text{Al}}$             | 0.182                     |
| (110)        | (110) | $(110)_{\text{SiC}} \parallel (110)_{\text{Al}}, [00\bar{1}]_{\text{SiC}} \parallel [00\bar{1}]_{\text{Al}}$ | 0.245                     |
| (110)        | (111) | $(110)_{\text{SiC}} \parallel (111)_{\text{Al}}, [00\bar{1}]_{\text{SiC}} \parallel [\bar{1}10]_{\text{Al}}$ | 0.144                     |
| (111)-C      | (100) | $(111)_{\text{SiC}} \parallel (100)_{\text{Al}}, [\bar{1}10]_{\text{SiC}} \parallel [010]_{\text{Al}}$       | 0.275                     |
| (111)-C      | (110) | $(111)_{\text{SiC}} \parallel (110)_{\text{Al}}, [\bar{1}10]_{\text{SiC}} \parallel [00\bar{1}]_{\text{Al}}$ | 0.205                     |
| (111)-C      | (111) | $(111)_{\text{SiC}} \parallel (111)_{\text{Al}}, [\bar{1}10]_{\text{SiC}} \parallel [\bar{1}10]_{\text{Al}}$ | 0.316                     |
| (111)-Si     | (100) | $(111)_{\text{SiC}} \parallel (100)_{\text{Al}}, [\bar{1}10]_{\text{SiC}} \parallel [010]_{\text{Al}}$       | 0.249                     |
| (111)-Si     | (110) | $(111)_{\text{SiC}} \parallel (110)_{\text{Al}}, [\bar{1}10]_{\text{SiC}} \parallel [00\bar{1}]_{\text{Al}}$ | 0.195                     |
| (111)-Si     | (111) | $(111)_{\text{SiC}} \parallel (111)_{\text{Al}}, [\bar{1}10]_{\text{SiC}} \parallel [\bar{1}10]_{\text{Al}}$ | 0.309                     |

An analysis of the calculated results reveals two general trends. The first is that the cohesive energy of Al/SiC-C interface is larger than that of the same Al/SiC-Si interface. This indicates that the Al-C interaction is stronger than the Al-Si interaction. This is in agreement with experimental observations<sup>2</sup> and other theoretical calculations.<sup>26</sup> This can be explained by the difference in the Al-Si and Al-C bond lengths.<sup>24,26</sup> The Al-Si bond length is much larger than the sum of covalent radii of Al and Si, indicating that the interaction between Al and Si does not have strong covalent character and is relatively weak. On the other hand, the Al-C bond length is very close to the sum of their covalent radii, suggesting a strong covalent character. The second trend is that for (110) and (111) surfaces of SiC, interfaces with Al of common indices have larger cohesive energies, while the same is not true for the SiC(100) surface. In fact, Al(111)/SiC(100)-(C or -Si) have a larger cohesive energy than that of the Al(100)/SiC(100)-(C or -Si). For the unreconstructed SiC (110) and (111) surfaces, it is expected that the best match will be with Al surfaces of common index on the basis of small-lattice misfit and high-bonded atom density and strength. Meanwhile, the dimerization on the SiC(100) surface, which certainly changes its bonding geometry and character, is considered the cause of the different situation at the interface of SiC(100) and Al. The present MD simulation is not able to provide a microscopic description of the nature of the bonding at the SiC/Al interfaces, which is necessary for a full understanding of the problem.

We also have analyzed the atomic configurations of all 15 Al/SiC interfaces. Figure 1 shows the atomic configuration of the Al(001)/SiC(001)-C interface before and after the relaxation. It is seen that the C atoms on the top layer of the SiC surface have strong movement from their free-surface positions and the underlayer atoms have little change in position. This can be understood as the result of the bonding of the surface C atoms with the contacting Al atoms. In this

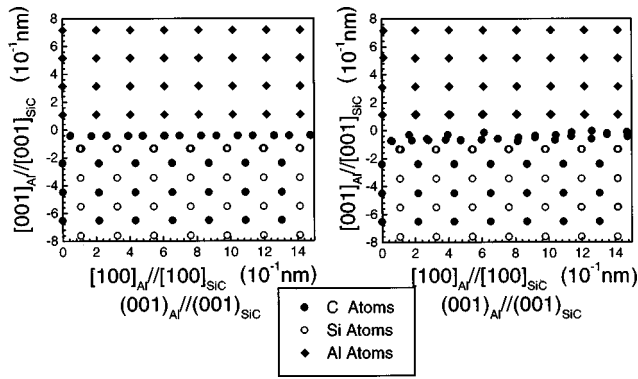


FIG. 1. Atomic configuration of the Al(001)/SiC(001)-C interface (a) before and (b) after relaxation.

process, the SiC(001) surface dimerization is at least partially removed and the SiC(100)-(2 $\times$ 1) reconstruction pattern is destroyed. Figure 2 shows the atomic configuration of the Al(001)/SiC(001)-Si interface. It is seen that the movement of the top-layer Si atoms is much smaller than that of the C atoms shown in Fig. 1. This is consistent with the above cohesive energy analysis that the Al-C interaction is stronger than the Al-Si interaction. Figures 3 and 4 show the atomic configurations of the interfaces of Al(100) with C- and Si-terminated SiC(111). It is seen again that the movement of C atoms is much stronger than that of Si atoms, even when C atoms are below Si atoms (see Fig. 4). Finally, Fig. 5 shows the atomic configuration of the interface between Al(100) and the nonpolar SiC(110) surface. The situation is the same as in other cases shown above with a strong C-atom movement and little Si-atom movement. In general, the movement of Al atoms is relatively small in all cases. It is also clear that the movement of interfacial atoms is smaller for the SiC(110) and SiC(111) surfaces, that show no surface reconstruction, than for the SiC(100) surface, that undergoes a (2 $\times$ 1) reconstruction through surface dimerization. In the former case, the nonreconstructed surface atoms only adjust the bond length within a small region to reach the stable structure while the reconstructed surface atoms in the latter case have to move over a larger distance to form the stable Al-C or Al-Si bonds.

Some general structural features of the Al/SiC interface are observed. The interaction between Al and SiC is only

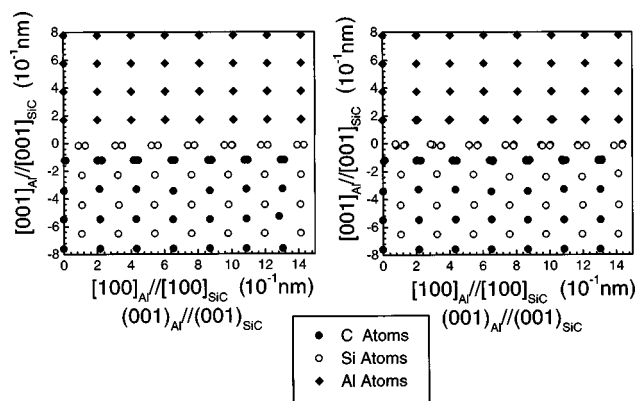


FIG. 2. Atomic configuration of the Al(001)/SiC(001)-Si interface (a) before and (b) after relaxation.

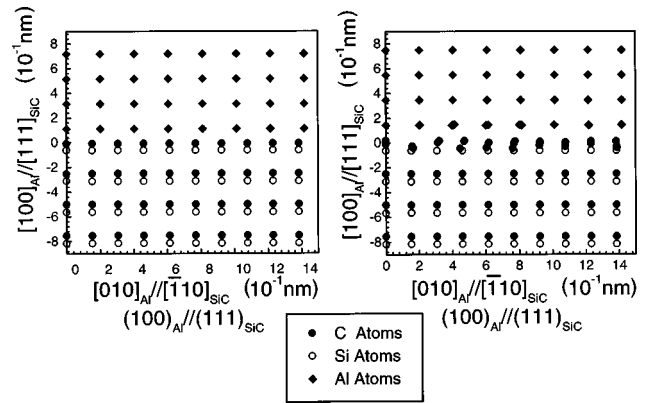


FIG. 3. Atomic configuration of the Al(100)/SiC(111)-C interface (a) before and (b) after relaxation.

limited to a narrow region (two or three atomic layers) near the interface. The interaction between Al and the second layer (C-terminated) or third layer (Si-terminated) atoms on the SiC side is quite weak. This is in good agreement with the result of electronic structure calculations.<sup>26</sup> It is also seen that Al atoms do not penetrate into SiC. This supports the conclusion of experimental<sup>2,12</sup> and other theoretical<sup>26</sup> work. The interface is divided into two crystal bulk parts with a definite orientation relationship separated by a narrow amorphous layer. This picture is in excellent agreement with experiment.<sup>14,15</sup> The situation here is similar to the grain boundary structure<sup>47-49</sup> and nanocrystalline silicon,<sup>50-52</sup> which are composed of crystalline grain interiors with an amorphous intergranular phase. This kind of metastable microstructure is typical for systems under severe constrain. In the case of Al/SiC interfaces obtained using squeeze casting method, atoms near the interface may be in a constrained state because of the high-applied pressure. Therefore, the system may not relax to the global minimum but a local minimum.<sup>13,14</sup> In the present model, only five Al layers were allowed to relax freely while others froze. This is a good model for a constrained system. It is expected that the structure composed of two crystalline parts connected by an amorphous layer is a common feature of the two-phase adhesion under constrained conditions. The amorphous structure seems to act as a stress buffer to tolerate the high stress.

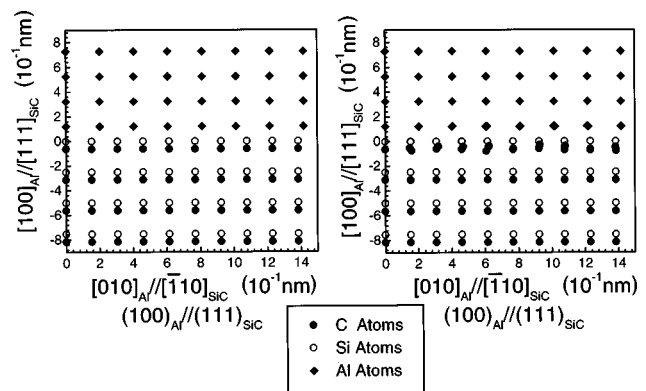


FIG. 4. Atomic configuration of the Al(100)/SiC(111)-Si interface (a) before and (b) after relaxation.

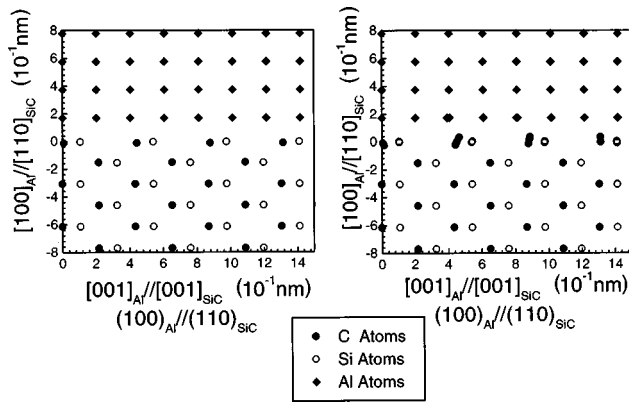


FIG. 5. Atomic configuration of the Al(100)/SiC(110) interface (a) before and (b) after relaxation.

### C. Deviation from ideal orientation relationships at the Al/SiC interface

There is experimental evidence<sup>21</sup> showing that many OR's at the Al/SiC interfaces do not satisfy ideal arrangement but have small deviations. Here we address this issue by constructing a series of Al/SiC interfaces with different relative orientations. It is achieved by rotating the Al bulk about the two axes normal and parallel to the interface. The rotation can be expressed in terms of the Euler angles  $\psi$  and  $\theta$ .

Figure 6 shows the calculated cohesive energy of the Al(100)/SiC(100)-C interface structure as a function of the Euler angles. It is seen that when the deviation of the angles from the ideal arrangement is not too large the cohesive energy decrease is very slow, suggesting a metastable region for non-ideal OR's at the Al/SiC interface. When the deviation becomes large, the cohesive energy decreases sharply as a function of the angles, indicating the structure is unstable.

## IV. SUMMARY

We have performed molecular-dynamics simulation with empirical interatomic potentials to study low-index Al/SiC interface structures. It is found that there is a positive correlation between the stability of a specific orientation relationship at the interface and its cohesive energy. It is also found that the Al-C interaction is stronger than Al-Si interaction in agreement with experimental observations and other theoretical calculations. It is seen that the structural change due to bonding between Al and SiC is limited to a narrow region near the interface, dividing the interface structure into two bulk crystal parts separated by an amorphous layer. This structure is similar to those found in large-angle grain boundaries and nanocrystalline silicon. Based on the cohesive energy analysis, it is found that the

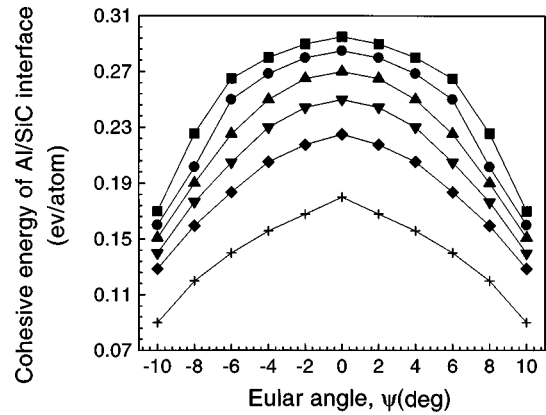


FIG. 6. Cohesive energy of the Al/SiC interface as function of the Euler angles. From top to bottom curve:  $\theta=0^\circ$ ,  $\theta=2^\circ$ ,  $\theta=4^\circ$ ,  $\theta=6^\circ$ ,  $\theta=8^\circ$ , and  $\theta=10^\circ$ .

orientation relationship is relatively stable when deviated from the ideal arrangement by a small rotation along the axis normal or parallel to the interface. It is predicted that more low-index Al/SiC interface structures should be experimentally observable, and many of these structures are expected to have orientation relationships different from the ideal arrangement.

The results presented in this paper provide a systematic understanding of the low-index Al/SiC interfaces. It is expected to have an impact on future work on the nature of adhesion between Al and SiC and on other metal/ceramic interfaces as well as various grain boundaries. It is noted that the present quantitative values and the details of atomic configurations may be subject to improvement by more accurate calculations. However, the physical picture and systematic trends found in this paper are expected to remain valid. Although the empirical molecular-dynamics simulation technique has its limitations in quantitative accuracy and microscopic mechanism, it does have the advantage of allowing the study of large supercells, thus better representing real-material systems and providing useful insight into the material property of complicated systems like composite interfaces. We hope that the present paper will stimulate further investigations of Al/SiC interfaces and other two-phase adhesion problems.

## ACKNOWLEDGMENTS

Xuan Luo thanks Professor Yuming Wang in Jilin University for his helpful discussion. This investigation was supported by the National Natural Science Foundation of China and the Pan Deng Project. Changfeng Chen was partially supported by the National Science Foundation under Grant No. OSR-9353227 and the Department of Energy under the EPSCoR program.

\*Also at China Center of Advanced Science and Technology (World Laboratory), P.O. Box 8730, Beijing, People's Republic of China.

<sup>1</sup>A. B. Anderson and C. Ravimohan, Phys. Rev. B **38**, 974 (1988).

<sup>2</sup>V. M. Bermudez, J. Appl. Phys. **63**, 4951 (1988).

<sup>3</sup>K. Yasuda, T. Hayakawa, and M. Saji, IEEE Trans. Electron Devices **ED-34**, 2002 (1987).

<sup>4</sup>T. M. Parrill and Y. W. Chung, J. Vac. Sci. Technol. A **6**, 1598 (1988).

- <sup>5</sup>K. M. Geib, C. W. Wilmsen, J. E. Mahan, and M. C. Bost, *J. Appl. Phys.* **61**, 5299 (1987).
- <sup>6</sup>C. S. Pai, C. M. Hanson, and S. S. Lau, *J. Appl. Phys.* **57**, 618 (1985).
- <sup>7</sup>I. Ohdomari, S. Sha, H. Aochi, T. Chikyow, and S. Suzuki, *J. Appl. Phys.* **62**, 3747 (1987).
- <sup>8</sup>S. Hasegawa, S. Nakamura, N. Kawamoto, H. Bishibe, and Y. Mizokawa, *Surf. Sci.* **206**, L851 (1988).
- <sup>9</sup>M. Van Den Burg and J. Th. M. De Hosson, *Acta Metall. Mater.* **40**, S281 (1992).
- <sup>10</sup>R. J. Arsenault and J. C. Romero, *Scr. Metall. Mater.* **32**, 1783 (1995).
- <sup>11</sup>J. C. Romero, L. Wang, and R. J. Arsenault, *Mater. Sci. Eng., A* **212**, 1 (1996).
- <sup>12</sup>L. Cao, L. Geng, C. K. Yao, and T. Q. Lei, *Scr. Metall.* **23**, 227 (1989).
- <sup>13</sup>L. Geng and C. K. Yao, *Scr. Metall. Mater.* **33**, 949 (1995).
- <sup>14</sup>Z. R. Liu, D. Z. Wang, and C. K. Yao, *J. Mater. Sci.* **31**, 6403 (1996).
- <sup>15</sup>R. J. Arsenault and R. M. Fisher, *Scr. Metall.* **17**, 67 (1983).
- <sup>16</sup>R. J. Arsenault and C. S. Pande, *Scr. Metall.* **18**, 1131 (1984).
- <sup>17</sup>L. Porte, *J. Appl. Phys.* **60**, 635 (1986).
- <sup>18</sup>C. Badini, *J. Mater. Sci.* **25**, 2607 (1990).
- <sup>19</sup>K. Saganuma, *J. Mater. Res.* **8**, 2569 (1993).
- <sup>20</sup>K. S. Foo, W. M. Banks, A. J. Craven, and A. Hendry, *Composites* **25**, 677 (1994).
- <sup>21</sup>Xuan Luo and Gefei Qian (unpublished).
- <sup>22</sup>Wenchang Lu, Ling Ye, and Kaiming Zhang, *Chin. Phys. Lett.* **9**, 101 (1992).
- <sup>23</sup>S. P. Mahandru and A. B. Anderson, *Surf. Sci.* **245**, 333 (1991).
- <sup>24</sup>S. Li, R. J. Arsenault, and P. Jena, *J. Appl. Phys.* **64**, 6246 (1988).
- <sup>25</sup>B. K. Rao and P. Jena, *Appl. Phys. Lett.* **57**, 2308 (1990).
- <sup>26</sup>W. C. Lu, K. M. Zhang, and X. D. Xie, *Phys. Rev. B* **45**, 11 048 (1992).
- <sup>27</sup>M. Kohyama, *Modell. Simul. Mater. Sci. Eng.* **4**, 397 (1996).
- <sup>28</sup>X. Hu, H. Yan, and F. S. Ohuchi, in *1994 Diamond, SiC and Nitride Wide Bandgap Semiconductors*, edited by C. H. Carter, Jr., G. Gildenblat, S. Nakamura, and R. J. Nemanich, MRS Symposia Proceedings No. 339 (Materials Research Society, Pittsburgh, 1994), pp. 15–20.
- <sup>29</sup>D. M. Bylander, L. Kleinman, and S. Lee, *Phys. Rev. B* **42**, 1394 (1990).
- <sup>30</sup>J. Tersoff, *Phys. Rev. B* **39**, 5566 (1989).
- <sup>31</sup>K. E. Khor and S. Das Sarma, *Phys. Rev. B* **38**, 3318 (1988).
- <sup>32</sup>T. Ito, K. E. Khor, and S. Das Sarma, *Phys. Rev. B* **40**, 9715 (1989).
- <sup>33</sup>T. Ito, K. E. Khor, and S. Das Sarma, *Phys. Rev. B* **41**, 3893 (1990).
- <sup>34</sup>J. Tersoff, *Phys. Rev. B* **38**, 9902 (1988); **39**, 5566 (1989).
- <sup>35</sup>X. Luo, G. F. Qian, W. D. Fei, E. G. Wang, and C. F. Chen, *Phys. Rev. B* **57**, 9234 (1998).
- <sup>36</sup>J. Tersoff (private communication).
- <sup>37</sup>J. R. Beeler, Jr., in *Computer Simulation in Material Science: Atomistic Model Computer Experiments*, edited by R. J. Arsenault, J. R. Beeler, Jr., and D. M. Esterling (ASM International, Metals Park, OH, 1988).
- <sup>38</sup>Xuan Luo, Gefei Qian, and Yuming Wang, *Acta Phys. Sin.* **43**, 1957 (1994).
- <sup>39</sup>Xuan Luo, Weidong Fei, Gefei Qian, and Yuming Wang, *Acta Metall. Sin.* **32**, 805 (1996).
- <sup>40</sup>L. Verlet, *Phys. Rev.* **159**, 98 (1967).
- <sup>41</sup>M. Kitabatake, P. Fons, and J. E. Greene, *J. Vac. Sci. Technol. A* **9**, 91 (1991).
- <sup>42</sup>J. R. Beeler, Jr., *Radiation Effects, Computer Experiments: Defect in Solids* (North-Holland, Amsterdam, 1983), p. 30.
- <sup>43</sup>L. Geng and C. K. Yao, *J. Mater. Sci. Technol.* **9**, 431 (1993).
- <sup>44</sup>N. K. Sharma, W. S. Williams, and A. Zangvil, *J. Am. Ceram. Soc.* **67**, 715 (1984).
- <sup>45</sup>X. Ning, Y. Lu, K. Hu, and H. Ye, *Chin. J. Mater. Sci. Technol.* **8**, 1 (1992).
- <sup>46</sup>Q. Liu, K. Wu, L. Geng, and C. K. Yao, *Mater. Sci. Eng., A* **130**, 113 (1990).
- <sup>47</sup>P. Keblinski, S. R. Philipot, D. Wolf, and H. Gleiter, *Phys. Rev. Lett.* **77**, 2965 (1996).
- <sup>48</sup>P. Keblinski, D. Wolf, S. R. Philipot, and H. Gleiter, *Phys. Lett. A* **226**, 205 (1997).
- <sup>49</sup>P. Keblinski, D. Wolf, S. R. Philipot, and H. Gleiter, *Philos. Mag. Lett.* **76**, 143 (1997).
- <sup>50</sup>R. W. Cahn, *Nature (London)* **390**, 344 (1997).
- <sup>51</sup>D. Wolf and K. L. Meikle, in *Materials Interfaces: Atomic-level Structures and Properties*, edited by D. Wolf and S. Yip (Chapman and Hall, London, 1992), pp. 87–150.
- <sup>52</sup>A. P. Sutton and R. W. Balluffi, *Interfaces in Crystalline Materials* (Oxford University Press, 1995), pp. 384–386.